

Large Area Nano-patterning by Masked Ion Implantation Using Anodic Porous Alumina

Masahide Nakamura¹, Seisuke Nigo² and Naoki Kishimoo²

¹Graduate School of Pure and Applied Sciences, University of Tsukuba
1-1-1, Tennohdai, Tsukuba, Ibaraki, 305-8571, Japan

²Quantum Beam Center, National Institute for Materials Science
3-13 Sakura, Tsukuba, Ibaraki, 305-0003, Japan

Large area nano-patterning has been conducted by masked ion implantation with anodic porous alumina. The purpose of this work is to develop a nano-patterning method leading to 3D control for device fabrication. Aluminum anodic oxidation is one of the best controllable self-assembling processes to fabricate large-area pore patterns. An anodic porous alumina was fabricated by two-step anodization process in 0.3 M oxalic acid and phosphoric acid. The two-step anodization process attained periodic porous arrays. The porous alumina was delaminated from the base aluminum by chemical etching and was mounted onto a crystalline SiO₂ substrate, removing the residual barrier layer by Ar sputtering. Subsequently, negative Cu ions of 60 keV were irradiated to the substrate. After the irradiation, surface morphology of the SiO₂ substrate was observed by SEM. The patterned irradiation was successfully conducted with the anodic porous-alumina mask to 1×10^{16} ions/cm². Beyond this tolerance limit, the pore size decreased with increasing ion fluence, because of ion-induced deformation. In order to reduce the deformation, we also employed Au or carbon coating on the mask surface. The carbon coating significantly improved the radiation resistance of the mask.

Key words: masked irradiation, anodic porous alumina, self-assembly, nano-patterning

1. INTRODUCTION

Ion irradiation techniques have been extensively used for materials modification and direct processing, such as impurity doping, ion milling, ion mixing, etc. The ion-based techniques have unique advantages:

- good controllability along the depth, by changing the incident energy of ions,
- non-equilibrium atomic injection beyond the thermodynamic restriction.
- short de Broglie wavelength, much shorter than those of photons or electrons.

By using such advantages, the ion irradiation techniques can be applied for various applications. Among the ion irradiation techniques, either ion projection lithography/patterning or masked irradiation has recently attracted much attention for large-area nano-patterning to fabricate device structures. In the case of ion projection, ions from the ion source pass the patterned stencil mask ($< 10^3$ eV), and are accelerated, via the beam column, up to the target energy (10 - 10^2 keV). On the other hand, the masked irradiation does not require such a sophisticated beam column, but the patterned mask is placed directly on the mask. Although the masked irradiation has the merit of simplicity, there are two drawbacks: One is the possible radiation damage on the mask at the higher ion energy. The other is higher requirements for the mask performance, e.g., accuracy in fabrication. For instance, to make a 100 nm feature, one has to prepare a mask of the same shape with enough accuracy, whereas the ion projection method of 1/10-contraction only requires 1 μ m-featured mask. Consequently, one of the most important issues for the masked irradiation is development of the high-performance mask.

In this work, we have attempted large area nano-patterning by the masked irradiation. We focus on the mask performance for the patterned irradiation.

To fabricate the patterned masks, one can usually employ electron-beam lithography, focused ion beam, scanning-probe writing and so on. These methods have good controllability, but are mostly of low throughputs and costly for the large-area patterning.

To prepare nm-featured masks, we have used anodic porous-alumina membrane as a self-assembled mask rather than a lithographic mask. The anodic porous alumina is well known as one of the most typical self-assembled nano-porous materials [1-3]. The self-assembling phenomenon is suitable for large area patterning. One of the most significant advantages of the anodic porous alumina is superb controllability of the interpore distance, pore diameter and thickness of the membrane, by changing the anodization conditions.

2. EXPERIMENTAL

2.1. Anodization and pore widening process

High-purity (99.99%) aluminum foils of 0.5 mm thick were used for anodization. First, aluminum foils were electro-polished in a mixture of HClO₄ and C₂H₅OH at -10°C to smoothen the surface. Subsequently, a two-step anodization process was carried out to obtain highly-ordered nanopore arrays [4]. The first anodization process was done at a constant voltage of 40 V in a 0.3 M oxalic acid solution at 20°C for 4.5 hours. After the first anodization, the porous alumina layer, whose pores were not yet well-organized, was mostly removed by dipping in a mixture of phosphoric acid and chromic acid at 60°C for 1 hour. The second anodization was carried out in a 0.3 M phosphoric acid solution at 20°C for 9 min. Finally, the pore size was increased by dipping in 0.5 M NaOH solution for 15 sec.

2.2. Fabrication of porous alumina masks

Fabrication processes of porous alumina masks are shown in Fig. 1. After the anodization, the porous

alumina membrane was separated from the aluminum foil by dipping into a saturated HgCl_2 solution, and was picked up with a SiO_2 substrate. The alumina membrane adheres to the SiO_2 substrate by van der Waals force when it dries out. At this stage, the pores did not pass through the membrane, since a thin Al_2O_3 barrier layer remained on the top side (ex-bottom side). The barrier layer was removed by Ar plasma sputtering.

In addition, either carbon of 30 nm thick or Au of 40 nm thick was deposited on the surface of the anodic porous alumina to improve the radiation resistance.

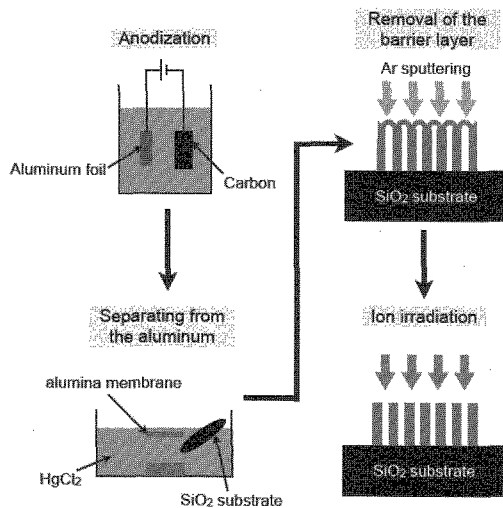


Fig. 1. Fabrication processes of the porous alumina mask.

2.3. Ion implantation

Negative Cu ions of 60 keV were irradiated at a current of $3 \mu\text{A}/\text{cm}^2$ to the crystalline SiO_2 substrate, through the anodic porous-alumina mask. Negative ions are effective to alleviate surface charging of the substrate under the irradiation. When ions are irradiated to an insulator (such as alumina), the surface of the sample is charged by accumulation of deposited ions. It becomes significant for nanopatterning by an ion irradiation technique. The ion fluences applied are 1×10^{16} , 2×10^{16} , 3×10^{16} ions/ cm^2 . After irradiation, the structural changes of the crystalline SiO_2 substrate were studied by AFM and SEM.

3. RESULTS

3.1. Mask fabrication

Fig. 2 shows the anodic porous alumina with an interpore distance of 100 nm, the pore diameter of 40 nm and the thickness of 270 nm. In the cross-sectional view of Fig 2 (b), which shows the bottom side of the alumina membrane after removal of the barrier layer, it is noted that the pores were opened through the thickness.

3.2. Application to EB-deposition

Next we demonstrated the mask performance by EB-deposition. The result of the Au deposition with the porous alumina mask is shown in Fig. 3. It is seen that the Au island arrays form on the SiO_2 substrate, transcribing the mask pattern. The Au islands are of the same size as that of the mask, about 40 nm. This result

demonstrates that the anodic porous alumina with through pores is applicable to masks for vacuum deposition.

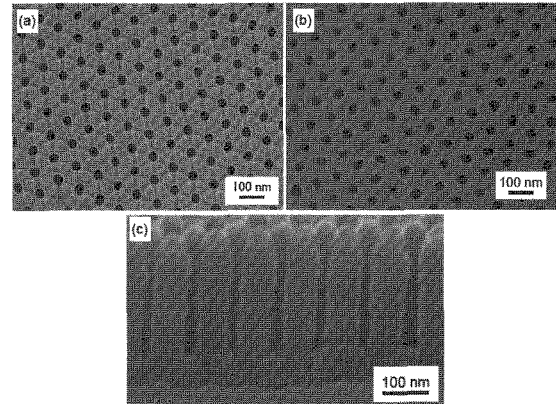


Fig. 2. Surface morphology of the anodic porous alumina, after two-step anodization (a), after removal of the barrier layer (b) and cross-section of anodic porous alumina (c).

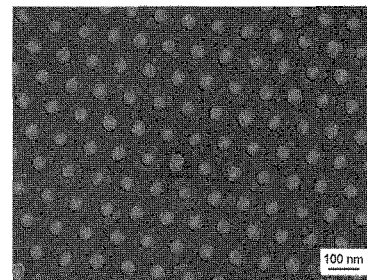


Fig. 3. SEM image of Au islands deposited on the SiO_2 substrate after removing the mask.

3.3. Surface morphology of crystalline SiO_2 substrate after irradiation

After ion irradiation of 2×10^{16} ions/ cm^2 , the surface of the crystalline SiO_2 substrate was observed by AFM (Fig 4). The ion irradiation to crystalline SiO_2 induces swelling. The swelling pattern is almost the same as the mask pattern, and the step height of swelling was about 5 nm. It demonstrates that the anodic porous alumina is applicable for ion irradiation, roughly up to this fluence.

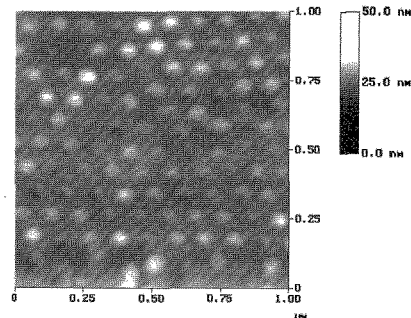


Fig. 4. Surface morphology of crystalline SiO_2 substrate after ion irradiation to 2×10^{16} ions/ cm^2 .

3.4. Mask performance against the ion irradiation

It has been demonstrated that nano-patterning by masked implantation is successfully conducted using

anodic porous alumina up to 2×10^{16} ions/cm². But, when we attempt to fabricate nanoparticles by ion implantation, the higher fluences of $\sim 10^{17}$ ions/cm² are demanded. It is thus necessary to study the radiation resistance at the higher fluences. Fig. 5 shows surface morphology of the anodic porous-alumina mask before and after irradiation. The pore size decreases with increasing ion fluence around 2×10^{16} ions/cm², and the pores are almost closed at a fluence of 3×10^{16} ions/cm². Fig. 6 shows the cross-sections of the same irradiation conditions. The shape of the pore wall changed like mushrooms near the top surface after the irradiation of 2×10^{16} ions/cm².

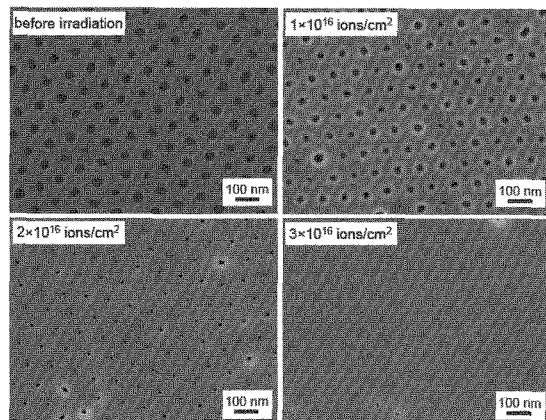


Fig. 5. SEM images of the anodic porous alumina mask before and after the ion irradiation.

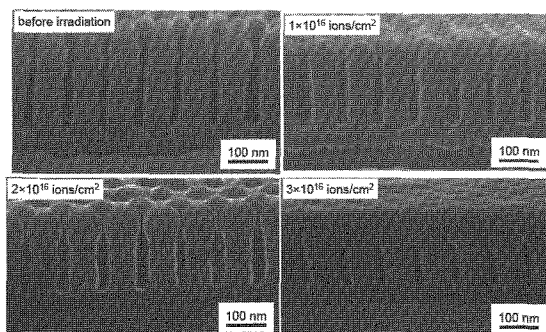


Fig. 6. Cross-sectional SEM images of the anodic porous alumina before and after irradiation.

This plastic deformation is a characteristic phenomenon in ion irradiation to Al₂O₃ or SiO₂. It has been reported that this deformation is mainly caused by electronic excitation [5-7]. The transverse deformation is hazardous to the mask performance and restricts the tolerant fluence.

It is consequently expected that metal coating on the surface will be effective against this phenomenon. First, we coated Au on the anodic porous alumina. Fig. 7 shows the mask surface with Au coating, before and after irradiation. While the pore size evenly decrease without coating, they unexpectedly changed as seen in SEM images of 1×10^{16} and 2×10^{16} ions/cm² with Au coating. The pores with the Au coating are closed at about 2×10^{16} ions/cm² and again appear at 3×10^{16} ions/cm². The Au layer coated on the anodic alumina is thus unstable on ion irradiation. It is judged from

these results that the Au coating is not suitable for protecting the anodic porous alumina.

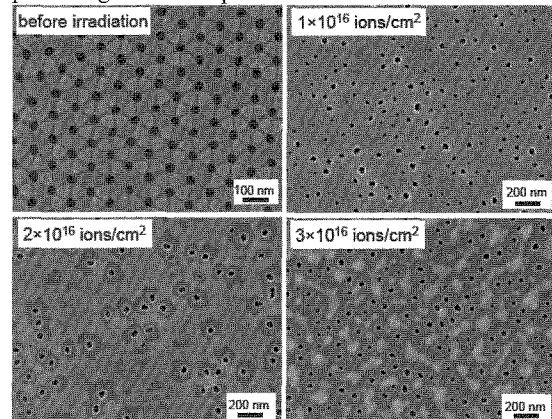


Fig. 7. SEM images of anodic porous alumina with Au coating, before and after the ion irradiation.

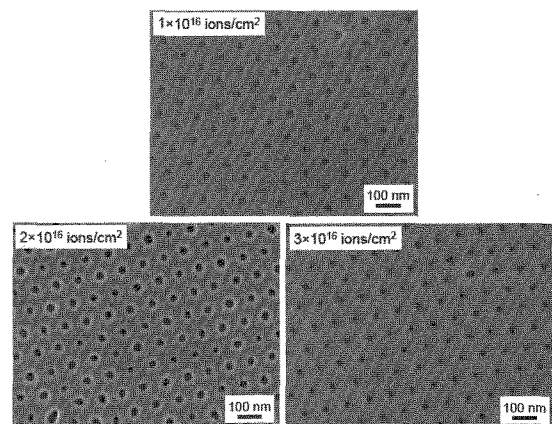


Fig. 8. SEM images of anodic porous alumina with C coating after irradiation.

Next, we attempted carbon coating on the mask surface. Fig. 8 shows the surface morphology of the carbon-coated porous alumina before and after the irradiation. The pore size is unchanged at around 2×10^{16} ions/cm² and begins decreasing at 3×10^{16} ions/cm². The mask performance is significantly improved.

Here, the carbon coating of 30 nm, adopted this time, was not enough thick to stop the ions irradiated, and the pore shrinkage may have been caused by the deformation of the base porous alumina. But clearly, carbon coating is effective to improve the radiation resistance of the mask, compared with the case of no coating. It is concluded that the anodic porous alumina with carbon coating is applicable for masked irradiation up to 3×10^{16} ions/cm².

4. DISCUSSION

It has been demonstrated that self-assembled nanopores of anodic porous alumina can be used for masked ion irradiation to make periodic nanopore arrays. We have presented the method of how to make a self-standing membrane of nanopores suitable for ion irradiation and have studied the radiation performance of the mask with ion fluence. One of the important merits of this nanopore system is fairly good controllability of the pore size and spacing, by changing the anodic

oxidation conditions (solution, voltage, time, temperature, etc.). We can apply this method to conduct periodically patterned nano-doping, nanoparticle patterning, photonic-crystal fabrication, magnetic patterning and so on. It should be noted that usage of self-assembled nanopores easily attains periodic wide patterns on a nano-scale, whereas other lithography-related methods are time-consuming.

The tolerant limit of ion fluence for 60 keV Cu ions was about 1×10^{16} ions/cm² for the porous alumina, which was determined by ion beam-induced plastic deformation. Within this tolerant fluence, we still have many applicable cases as mentioned above. The tolerant fluence should be a function of ion species and ion energy. If the ion-beam-induced deformation is dominated by the electronic excitation effect, it is speculated that the lighter or higher-energy ions are subject to lowering the tolerance. Further study is necessary to verify the tolerance limit for specific ion beams of concern.

As for improvement of the tolerance limit by coating, the carbon coating exhibited a good performance. The Au coating was unexpectedly worse. Hereafter, the differences between Au and C coatings are discussed. First, one of possible concerns is the surface temperature during ion irradiation and the thermally-induced change. The surface temperature can be roughly estimated by a balance between the input ion energy and the black body radiation. The steady-state temperature at the surface is estimated to be about 450 K, which is much lower than the melting point of Au or C. The ion-induced drastic change of Au coating is not due to thermal melting, at least. One of the other possible mechanisms is ion beam-induced sintering. Under ion irradiation, many vacancies are produced and anomalous vacancy diffusion can be enhanced under the ion irradiation even at room temperature. The irradiation-enhanced diffusion may result in sintering-like deformation under the irradiation.

Here, we discuss on the vacancy diffusion. First, the self-diffusion coefficients at 450 K (possible maximum temperature) are estimated to be 3.3×10^{-22} cm²/sec and 4.1×10^{-79} cm²/sec for Au and C, respectively. This difference arises from the activation energy of each material. The activation energies of Au-Au and C-C are 42.26 kcal/mole [8] and 163 kcal/mole [9], respectively. The larger activation energy of C-C is due to the tighter covalent bonding than the metallic bonding of Au-Au.

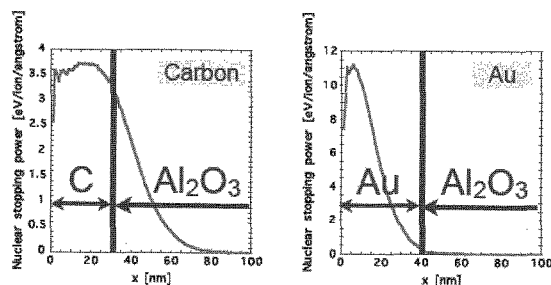


Fig. 9. Nuclear stopping power in C- and Au-coated Al₂O₃: with C coating of 30 nm (left) and with Au coating of 40 nm (right).

Fig. 9 shows nuclear stopping powers of C and Au coatings, calculated by the SRIM code. The number of vacancies produced in the Au layer is three times larger than that in the C layer. Both the thermal diffusion constant and the non-thermal vacancy density indicate that vacancy diffusion of Au is much larger than that of C under irradiation. It is consequently suggested that the drastic morphology change of the Au coating may be ascribed to the ion beam-induced sintering.

5. CONCLUSIONS

We have developed a method of how to make a self-standing mask membrane of nanopores suitable for ion irradiation and have demonstrated applicability to not only masks for EB-evaporation but also wide-area masks for patterned ion implantation.

For the mask fabrication, we employed the two-step anodization method to fabricate porous alumina and succeeded in fabricating a self-standing membrane of 270 nm thick with periodically-arrayed nanopores of 40 nm, after removing the barrier layer by Ar sputtering. The mask could be mounted directly onto the SiO₂ substrate and used for patterned irradiation.

The performance of the anodic porous-alumina mask was firstly demonstrated by EB-deposition and an ordered array of Au islands was successfully fabricated.

The mask performance for ion irradiation was studied by applying negative Cu ions at 60 keV to crystalline SiO₂ substrates. The patterned surface-swelling demonstrated effectiveness of the masked ion irradiation with the anodic porous alumina.

Deterioration of the porous alumina mask is caused by shrinkage of pore size, associated with ion-induced deformation. The fluence dependence of the surface morphology clarified the tolerance limit to be 1×10^{16} ions/cm² in the case of 60 keV Cu ions. This irradiation-induced plastic deformation was significantly decreased by carbon coating on the surface of the anodic porous alumina. As a result, the tolerance limit of the anodic porous alumina with carbon coating was significantly extended to 3×10^{16} ions/cm².

ACKNOWLEDGMENTS

A part of this study was financially supported by the Budget for Nuclear Research of the MEXT, based on the screening and counseling by the Atomic Energy Commission.

- [1] H. Masuda and K. S. Fukuda, *Science* 268 (1995) 1466.
- [2] S. Shingubara and J. Nanoparticle Res. 5 (2003) 17.
- [3] A. P. Li, F. Muller, A. Birner, K. Nielsch and U. Gosele, *J. Appl. Phys.* 84 (1998) 6023
- [4] H. Masuda and M. Satoh, *J. Appl. Phys.* Vol. 35 (1996) pp. L 126
- [5] T. van Dillen, A. Polman, P. R. Onck and E. van der Giessen *Phys. Rev. B* 71 (2005) 024103
- [6] T. van Dillen, E. van Giessen, P. R. Onck and A. Polman, *Phys. Rev. B* 74 (2006) 132103
- [7] E. Snoeks, T. Weber, A. Cacciato and A. Polman, *J. Appl. Phys.* 78 (1995) 4723
- [8] H. M. Gilder and D. Lazarus, *J. phys. Chem. Solids* 26 (1965) 2081
- [9] M. A. Kanter, *Phys. Rev.* 107 (1957) 655